Title

Rational Construction of Porous Metal—Organic Frameworks for Uranium(VI) Extraction: The Strong Periodic Tendency with a Metal Node

Journal

ACS Applied Materials & Interfaces, 12(12)

ISSN

1944-8244

Authors

Zhang, Zhi-Hui

Lan, Jian-Hui

Yuan, Li-Yong

et al.

Publication Date

2020-03-25

DOI

10.1021/acsami.0c02121

Peer reviewed

Rational Construction of Porous Metal–Organic Frameworks for Uranium(VI) Extraction: The Strong Periodic Tendency with a Metal Node

Zhi-Hui Zhang, Jian-Hui Lan, Li-Yong Yuan,* Pan-Pan Sheng, Ming-Yang He, Li-Rong Zheng, Qun Chen, Zhi-Fang Chai, John K. Gibson, and Wei-Qun Shi*

ABSTRACT: Although metal–organic frameworks (MOFs) have been reported as important porous materials for the potential utility in metal ion separation, coordinating the functionality, structure, and component of MOFs remains a great challenge. Herein, a series of anionic rare earth MOFs (RE-MOFs) were synthesized via a solvothermal template reaction and for the first time explored for uranium(VI) capture from an acidic medium. The unusually high extraction capacity of UO_2^{2+} (e.g., 538 mg U per g of Y-MOF) was achieved through ion-exchange with the concomitant release of $Me_2NH_2^+$, during which the uranium(VI) extraction in the series of isostructural RE-MOFs was found to be highly sensitive to the ionic radii of the metal nodes. That is, the uranium(VI) adsorption capacities continuously increased as the ionic radii decreased. In-depth mechanism insight was obtained from molecular dynamics simulations, suggesting that both the accessible pore volume of the MOFs and hydrogen-bonding interactions contribute to the strong periodic tendency of uranium(VI) extraction.

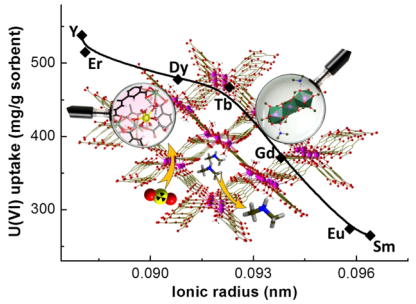

INTRODUCTION

Metal–organic frameworks (MOFs), with their well-ordered pore structures and tunable surface chemistry, offer a new platform for developing versatile materials for various applications in gas storage,[1] separations,[2−10] catalysis,[11] drug delivery,[12] and others, such as detoxification.[13] Among the MOF family, lanthanide-based MOFs (Ln-MOFs) represent an important subclass for their unique optical and magnetic function.[14−16] Meantime, their applications in adsorption/separation of gas, dyes, and volatile organic compounds[17−20] have been extensively expanded because of the porosity merits by judicious choices of organic linkers.

Lanthanides possess similar atomic radii and, therefore, comparable chemical properties, which lead to analogous Ln-MOFs network structures and properties when formed with particular ligands.[21] Up to now, however, the question of whether or not the periodic tendency of the Ln elements[22] correlates with the porosity, adsorbability, and selectivity of the resultant Ln-MOFs has not been addressed. Taking advantage of the subtle differences of the lanthanides for the construction of Ln-MOFs frameworks with a goal of a specific application remains a great challenge. This inspired us to characterize the relationship between the periodic properties of the series of lanthanide ions and the mechanism of Ln-MOFs in the realm of solid-phase extraction of metal ions. To achieve this aim, a series of anionic Ln-MOFs were employed because charged MOFs accommodating extra framework ions exhibit substantial ion-exchange ability like ion-exchange resins.[23] Given the possibility of solvent hydrolysis of polar aprotic solvents, such as dimethylformamide (DMF) and diethylformamide, it is plausible to synthesize anionic MOFs through the templating of $MeNH_3^+$, $Me_2NH_2^+$, or $Et_2NH_2^+$ cations.[23,24] Then, by tailoring the MOFs nodes across lanthanides, the influence of the so-called lanthanide contraction (different metal nodes) on the adsorption/ion-exchange behaviors of Ln-MOFs adsorbents could be addressed. In terms of adsorbates, uranium was used here as the representative of heavy metal ions.

As well known, with the widespread use of nuclear energy worldwide, separation of uranium is becoming a topic of great interest from the point of view of both reasonable utilization of uranium resources and environmental protection.[25,26] The linear uranyl (UO_2^{2+}) dication and its complexes dominate the environmental chemistry of uranium, and are universal in nature with a flexible coordination pattern involving four to six ligands in its equatorial plane,[27] which offers effective

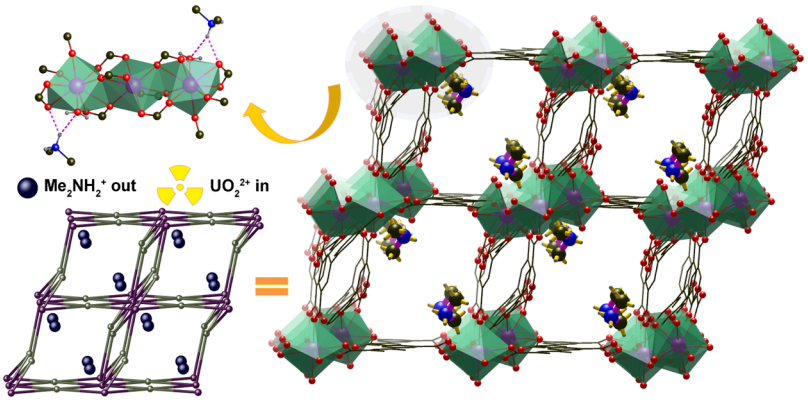

Figure 1. Structural representations of RE-MOFs depicting ion-exchange of UO_2^{2+} and $Me_2NH_2^+$.

opportunities for solid-phase extraction of uranium by taking advantage of ligand coordination.[28−30] Recently, many porous adsorbents built by functional ligands have been widely investigated ranging from porous organic polymers,[30−34] covalent organic frameworks[35−37] to MOF[38−43] materials for uranium sequestration.[44] The most reported MOF-type uranium(VI) adsorbents focused on the ligand modification of classical MOFs materials, such as Cu-BTC (HKUST-1),[45] MOF-76,[46] MIL-101,[47,48] UiO-66,[49,50] UiO-68,[51] and Zn-MOF-74.[52,53] Fluorescent platforms of terbium-MOF, constructed by carboxylate ligands containing N donors, have also been introduced for the convenient and quantified detection of uranium in complicated water environments containing possible competing metal ions.[46,54,55] In all these studies, however, the influence of metal nodes on the adsorption has never been disclosed.

Accordingly, we initiated the investigation on the adsorption/ion-exchange performances of anionic Ln-MOFs possessing inherent advantages in separation of uranium(VI) ions. A series of isostructural anionic Ln-MOFs and a Y-MOF as a rare earth (RE) MOF for comparison were synthesized based on a tetracarboxylic acid ligand through the templating of cationic dimethylammonium, where dimethylammonium was derived from acidic hydrolysis of the DMF solvent. These RE-MOFs (RE = rare earth) possess notable adsorbability toward uranium(VI) and show clear ion-exchange characteristics. Most importantly, although the lanthanide contraction merely leads to a 0.15 Å decrease in ionic radii across the entire lanthanide series and only an approx. 0.01 Å decrease between adjacent elements,[56] the resultant Ln-MOFs show significantly different U adsorption behavior. Specifically, together with Y-MOF, the crystalline isostructural RE-MOFs show a strong periodic tendency on the uranium(VI) extraction, which is well consistent with the intrinsic trend of related ionic radii of metal nodes. To the best of our knowledge, this is the first report of the metal node effect on the metal ion adsorption by MOFs.

EXPERIMENTAL SECTION

Caution! Although depleted uranium was used in these studies, precautions for handling radioactive materials must be followed, including proper worker training and special facilities.

Preparation of RE-MOFs. All RE-MOFs (RE = Sm, Eu, Gd, Tb, Dy, Er, Y) were synthesized according to a modification of a previously reported procedure,[57] with a typical synthesis protocol given for the Er-MOF, $(Me_2NH_2)_2[Er_3(H_{0.5}BPTC)_2(BPTC)(H_2O)_2]\cdot 2DMF\cdot 5H_2O$, where H_4BPTC is 3,3′,5,5′-biphenyltetracarboxylic acid. A mixture of Er_2O_3 (9.6 mg, 0.025 mmol), H_4BPTC (16.5 mg, 0.05 mmol), DMF (3 mL), ethanol (2 mL), and aqueous HCl (0.05 M, 2 mL) was transferred to a 23 mL Teflon-lined autoclave and heated under autogenous pressure at 140 °C for 4 days, and then slowly cooled to room temperature over a period of 3 days. The resulting pink sheet crystals were washed with distilled water three times. Yield: ∼60%, based on H_4BPTC.

Uranium(VI) Extraction Experiments. Adsorption of uranium(VI) was performed in a pH range of 2.5−5.0 using a batch method with an initial uranium(VI) concentration from 5 to 600 mg L^{-1}. The solid−liquid experiment was repeated at least three times for each adsorption data with the uncertainty within 5%. In a typical experiment, 4 mg of sorbent was added to 10 mL of uranium(VI) solution in a flask (i.e., 0.4 g sorbent/L). The solution pH was adjusted using a small volume of dilute HNO_3 or NaOH. The sorbent/solution mixture was stirred at room temperature before separating the solid phase from the solution using a 0.22 μm nylon membrane filter. The solutions were suitably diluted before analysis of the U concentration by ICP-OES. Control experiments were performed using the identical uranium(VI) solutions in the absence of sorbent. Detailed experimental procedures are shown in the Supporting Information (Sections S3−S4).

EXAFS Data Collection and Analysis. EXAFS spectra of the U-loaded samples at the U-L_{III} edge (17 166 eV) were recorded in fluorescence mode in the range of 17.0−17.9 keV at beamline 1W1B of the Beijing Synchrotron Radiation Facility (BSRF). A silicon (111) double-crystal monochromator was used to tune the incident X-ray beam to the desired energy. An yttrium foil (K-edge 17 038 eV) was simultaneously measured in transmission mode for energy calibration of the monochromator.

Molecular Dynamics Simulations. The van der Waals interaction of the MOF framework atoms was described by a Lennard-Jones potential with parameters from the universal force field.[58] For the uranyl cation, the Lennard-Jones potential parameters developed by Pomogaev et al.[59] were used. The simple point charge (SPC/E) water model[60] was used for the solvent water molecules, and the SHAKE algorithm was applied to fix their geometry.[61] The particle mesh-Ewald method was used to treat long-range electrostatic interactions. The main framework of the host material was kept rigid during all simulations, with the exception of dangling carboxyl groups, to enable coordination with guest species such as uranyl and water. Detailed methods and results are listed in the Supporting Information (Sections S11 and S12).

RESULTS AND DISCUSSION

Structures and Characterizations of RE-MOFs. Solvothermal reactions of RE oxides and 3,3′,5,5′-biphenyl tetracarboxylic acid (H_4BPTC) under acidic conditions in DMF/EtOH/H_2O mixed solvents resulted in a series of anionic RE-MOFs with uniform coordination frameworks, templated by in situ generated dimethylammonium cations from the hydrolysis of DMF in an acidic environment (Figure

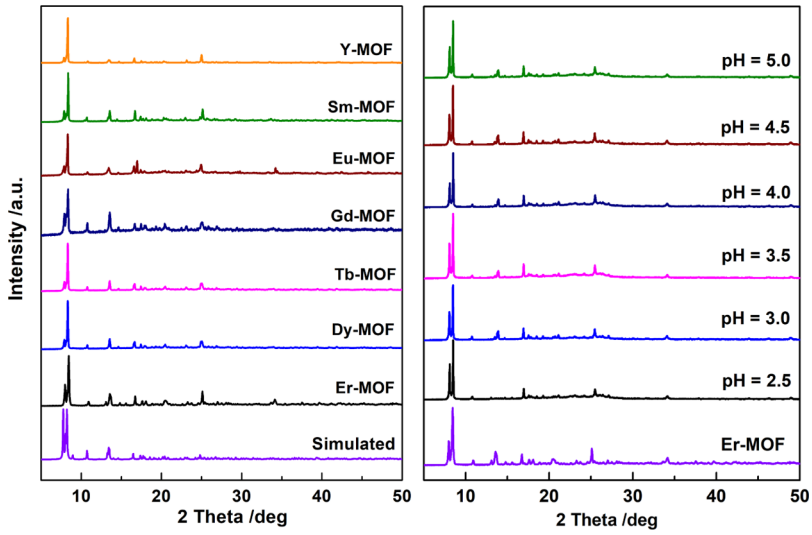

Figure 2. PXRD patterns of all prepared RE-MOFs (left) and an Er-MOF before and after uranium(VI) adsorption at various pH (right).

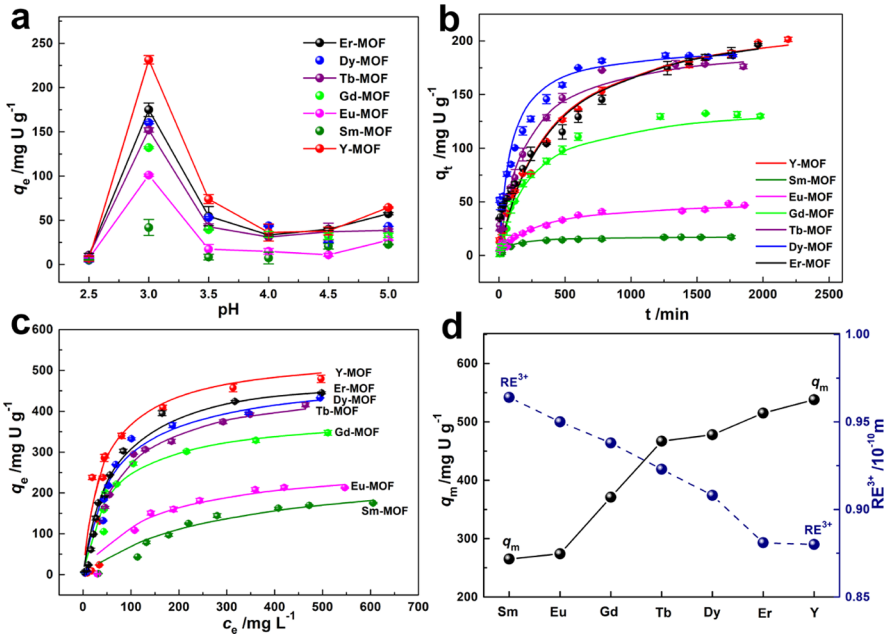

Figure 3. (a) Effect of pH on uranium(VI) adsorption, t = 24 h, c_0 = 100 mg L^{-1}. (b) Adsorption kinetics curves for uranium(VI) removal at pH = 3.0 ± 0.1, c_0 = 100 mg L^{-1}. (c) Plot of adsorption isotherms of uranium(VI) cations with adsorption amounts (q_e) vs equilibrium uranium(VI) concentration. (d) Relationship of ionic radii with the maximum uranium(VI) uptake capacities (q_m) at pH = 3.0 ± 0.1. Conditions for all data: $c_{adsorbent}$ = 0.4 g/L; T = 25 ± 0.5 °C.

1). Single-crystal X-ray diffraction (SCXRD) analysis reveals the composition of the RE-MOFs as $(Me_2NH_2)_2[Ln_3(H_{0.5}BPTC)_2(BPTC)(H_2O)_2]$·guests (Ln = Sm, Eu, Gd, Tb, Dy, Er; guests = $6H_2O$, $14H_2O$, $5H_2O$, $7H_2O$, $6H_2O$, $2DMF·5H_2O$, respectively) and $(Me_2NH_2)_2[Y_3(H_{0.5}BPTC)_2(BPTC)(DMF)_2]·2H_2O$. Despite differing terminal ligands (H_2O for Ln-MOFs vs. DMF for Y-MOF), all the RE-MOFs crystallize in the triclinic $P\bar{1}$ space group with very similar unit cell parameters (Table S1) and show 3D open anionic frameworks containing 1D channels (ca. 11 × 13 $Å^2$) along the crystallographic b axis that accommodate the counter cationic dimethylammonium and solvent guests (Figure 1). PLATON calculations[62] indicate ~40% solvent-accessible channel volumes of the unit cells.

The structures reveal that the coordination unit is a trinuclear cluster containing two crystallographically distinct RE ions. In one coordination motif, the RE^{3+} is eight-coordinated by eight oxygen atoms from six tetracarboxylate ligands, whereas in the other it is nine-coordinated by eight carboxylate oxygens and an oxygen atom from water. The dimethylammonium N atoms form strong hydrogen-bonding interactions with the carboxylates and the coordinated water ligands of the trinuclear cluster unit in the host frameworks (Figure S1). As a result of strong coordination and hydrogen-bonding interactions, all RE-MOFs are insoluble and remain intact in common solvents such as acetone, alcohols, DMF, and water.

Similar 3D anionic Ln-MOFs,[57,63] including a Eu-MOF[63] capable of fluorescent pH sensing and dye degradation, were

prepared by hydronium templating; the exclusion of bulky dimethylammonium may be a result from modest solvothermal temperatures and/or lower acidity. We have developed a facile synthesis strategy of RE-MOFs using RE_2O_3 as the metal ion source, with effective inclusion of dimethylammonium achieved by adjusting temperature and pH. Specifically, under acidic condition in the temperature range of 140−160 °C, reactions of RE_2O_3 and H_4BPTC provided a series of isostructural RE-MOFs with inclusion of dimethylammonium cations and solvent molecules. The dimethylammonium moieties reside in the large anionic channels along the [010] direction, providing a potential route for uranium(VI) cation uptake by ion-exchange. The coordination environments of the RE ions within the isostructural RE-MOFs are essentially equivalent such that comparison of extraction capacities should provide a correlation with ionic radii of the RE^{3+} cations.

Uranium(VI) Extraction Studies. To evaluate the RE-MOFs for uranium(VI) capture, batch adsorption experiments were performed (see the Supporting Information). Prior to adsorption, chemical activation of the MOFs with dichloromethane (CH_2Cl_2) removed uncoordinated and/or coordinated solvent molecules.[64] The formulas of the MOFs after chemical activation in Table S1 were obtained by elemental analysis. Thermal stability of the activated samples up to 360 °C (Figure S2) ensures practical adsorption applications under realistic high-temperature conditions. Powder XRD (PXRD) patterns confirm phase purity and stability of the activated crystalline RE-MOFs before and after uranium(VI) uptake at pH ≥ 3.0 (Figures 2 and S3−S8).

Uranium(VI) extraction was found to vary in the pH range of 2.5−5.0. All RE-MOFs achieved a maximum uranium(VI) adsorption (q_e, mg g^{-1}) at pH = 3.0 (Figure 3a), as was similarly found for MOF-76,[46] Fe^0@UiO-66-COOH,[40] and Fe_3O_4@ZIF-8 nanocomposites.[65] The adsorption kinetics for all the RE-MOFs (Figure 3b) can be well modeled by pseudo-second-order kinetics (Figure S9 and Table S2), which indicates chemiadsorption.[66,67] Similar kinetics for a chalcogenide material templated with organic ammonium cations revealed an ion-exchange mechanism for uranium(VI) ions.[67] Generally, the pH-induced uranium(VI) adsorption capacities of pristine MOF adsorbents are attributed to the synergic effect of the dissociative processes of metal cores and the protonation sites of the functional ligands.[39] In this case, the removal percentages of uranium(VI) by all RE-MOFs are relatively low at pH < 3.0, which may be due to the protonation of the active carboxylate sites and the part dissolution of the RE-MOFs in a more acidic aqueous solution. However, a higher pH value (>3.0) is not in favor of the ion-exchange process because of the dissociation of dimethylammonium, leading to the considerably decreased capacities for the recovery of uranium(VI).

As expected, adsorption isotherms for initial uranium concentrations from 5 to 600 mg·L^{-1} indicate continuous enhancement of uranium(VI) adsorption for all the RE-MOFs with increasing of the initial uranium concentration (Figure 3c). Interestingly, the uranium(VI) adsorption capacity continuously increased as the ionic radii of RE^{3+} nodes in the MOFs decreased (Figure 3d). This trend occurs over the pH range 3.0−5.0, with the maximum effect at pH 3.0. When the adsorption data are fitted to Langmuir and Freundlich models (Figure S10 and Table S3), it is apparent that there is a better fit to the Langmuir isotherm model, which indicates a monolayer adsorption process.[46] The maximum uranium(VI) adsorption capacities (mg/g) of the Ln-MOFs are 265 (Sm), 274 (Eu), 371 (Gd), 467 (Tb), 478 (Dy), and 515 (Er), respectively. The highest capacity is 538 mg/g for Y-MOF, which has the smallest metal ion nodes among the studied RE-MOFs. At the same time, it must be noted that the smallest atomic weight of Y-MOF also contributes to its largest adsorption capacity, supported by the thermal gravimetric result (Figure S2). However, to the best of our knowledge, the uranium(VI) adsorption capacity for Y-MOF represents one of the largest values for uranium(VI) capture by MOFs.

Uranium(VI) Uptake Mechanism. To understand the correlation between uranium(VI) adsorption and ionic radii of the RE^{3+} node, the uranium(VI) adsorption mechanism was assessed by recording scanning electron microscopy (SEM), XRD, Fourier transform infrared, ^1H NMR, and extended X-ray adsorption fine structure (EXAFS) spectra of U-loaded RE-MOFs. SEM images show the intact U-exchanged RE-MOFs (Figure S11). The comparison of PXRD patterns of dry samples with wet samples reveals no discernible changes, whereas the unit cells for a U-loaded Tb-MOF as evidenced by SCXRD are slightly smaller than its original parameters with a 1.57% volume decrease, which show some flexibility of the crystals in line with the triclinic $P\bar{1}$ space group.

IR spectra (Figures 4a and S12−S17) reveal that the weak resonance of the dimethylammonium C−H bonds of activated

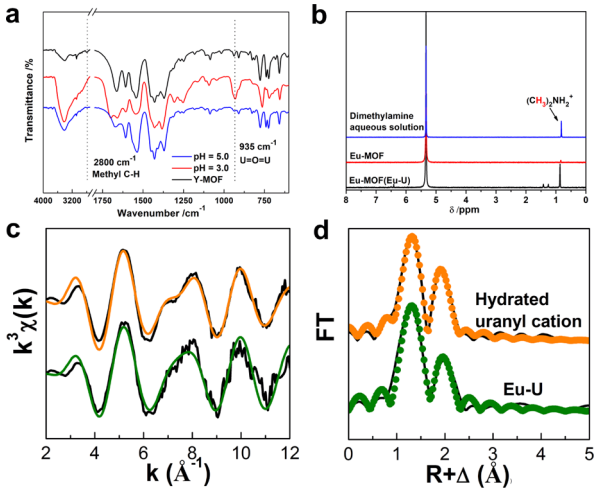

Figure 4. (a) IR spectra of Y-MOF before and after uranium(VI) adsorption at various pH. (b) ^1H NMR spectra of filtrates of Eu-MOF treated by a DCl solution with and without uranium(VI). Eu-MOF (Eu-U) and Eu-MOF denote the filtrates with and without uranium(VI), respectively. (c) EXAFS spectra of a U-loaded Eu-MOF (Eu-U), compared with uranium(VI) in aqueous solution. (d) Fourier-transformed space (R space) spectra of Eu-U, compared with uranium(VI) in aqueous solution.

RE-MOFs, centered around 2800 cm^{-1}, disappeared after uranium(VI) extraction, indicating the release of $Me_2NH_2^+$ cations during the uranium(VI) adsorption. The sharp O═U═O antisymmetric vibration at 935 cm^{-1} was more intense for pH = 3.0 than pH = 5.0, in accord with higher adsorption capacity at pH = 3.0. A significant red shift of uranyl on comparing it with free uranyl pentahydrate cations (963 cm^{-1}) indicates that the hydrated uranyl ion may have strong interactions with the host frameworks. The ion-exchange mechanism is further supported by ^1H NMR spectroscopy, which indicates release of $Me_2NH_2^+$ upon uranium(VI)

Table 1. Bond Parameters of U−O Obtained from EXAFS Data

sample	bond type[a]	coordination number	bond length R (Å)	bond disorder $\sigma^2 \times 10^{-3}$ (Å^2)	R factor
hydrated uranium	$U-O_{ax}$	2 (fixed)	1.76 ± 0.02	2.0 ± 0.3	0.007
	$U-O_{eq}$	5.0 ± 0.4	2.41 ± 0.02	7.5 ± 0.6	
Eu-U[b]	$U-O_{ax}$	2 (fixed)	1.77 ± 0.02	0.9 ± 0.6	0.009
	$U-O_{eq}$	4.5 ± 0.5	2.40 ± 0.02	8.0 ± 0.8	

[a]ax = axial; eq = equatorial. [b]Eu-U is a U-loaded sample of Eu-MOF.

adsorption. As seen in Figure 4b, the characteristic resonance of dimethylammonium was observed in the aqueous phase following uranium(VI) uptake by Eu-MOF, whereas it was not apparent in the aqueous phase in the absence of uranium(VI). Additionally, the uranium(VI) adsorption experiment in the presence of carbonate anions at a higher pH scope (8−10) turns out almost no adsorption of anionic uranium complexes, which conforms to the ion-exchange mechanism between cationic uranium hydrates and dimethylammonium for the anionic RE-MOFs.

EXAFS measurement of a U-loaded sample of Eu-MOF (Eu-U) gives similar spectra (Figure 4c,d) and almost the same metric parameters (Table 1) as obtained for uranium(VI) in aqueous solution. This is a clear indication that the coordination of uranium(VI) in Eu-MOF is evidently very similar to that of uranium(VI) in aqueous solution, supporting the above conclusion that uranium(VI) uptake in the Eu-MOF mainly occurs by an ion-exchange process between $Me_2NH_2^+$ and hydrated uranyl cations.

Considering all the above results, it is apparent that an ion-exchange mechanism is operative for uranium(VI) extraction by RE-MOFs. It is postulated that the regular variation of uranium(VI) adsorption as a function of ionic radii of the RE^{3+} node can be rationalized based on the accessible pore volume and hydrogen-bonding interactions between a $Me_2NH_2^+$ guest and framework host. In particular, a smaller ionic radius at the node results in a larger accessible pore volume and weaker hydrogen-bonding interactions between $Me_2NH_2^+$ and the MOF framework, which evidently leads to more facile displacement of $Me_2NH_2^+$ and thus more effective uranium(VI) adsorption.

Molecular Dynamics Simulations. To assess the above-postulated rationale for the correlation between uranyl adsorption and RE^{3+} radius, molecular dynamics (MD) simulations based on crystal structure data were performed to obtain accessible surface area, free pore volume, and maximum and limiting pore diameters of the RE-MOFs (Table S4). Examination of the hydrogen-bonding interactions in RE-MOFs reveals strong N−H···O interactions between the dimethylammonium cations and carboxylate oxygen atoms for most of the Ln-MOFs, but weak C−H···O interactions in Y-MOF (Figure S1), which rationalizes the exceptional ion-exchange ability of Y-MOF. Besides, in accord with its particularly high uranium(VI) uptake, Y-MOF exhibits the largest free volume of 0.29 cm^3/g and the highest accessible surface area of 558 m^2/g (Table S4). For the Ln-MOFs, despite similar Ln^{3+} radii and seemingly irregular hydrogen-bonding interactions, the correlation between free volume and adsorption capacity is partially reproduced; the relationships between free volumes is Er-MOF > Dy-MOF > Gd-MOF, and Tb-MOF > Eu-MOF, suggesting that accessible pore volumes may play a crucial role in the efficiency of uranyl adsorption in these MOFs. Anyway, we believe that the node effect is the result of several factors (e.g., hydrogen-bonding interactions, accessible pore volumes, atomic weight as mentioned above) acting together rather than being controlled by a single factor.

Based on all-atom MD simulations, the microscopic process of uranyl binding to RE-MOF can be modeled at the molecular level (MD details are in the Supporting Information). Considering Er-MOF as an example, eight uranyl cations were placed in a 2 × 2 × 2 supercell in the initial triclinic simulation box to obtain reasonably representative sampling, which furthermore yields a neutral simulation box. Figure 5a presents a snapshot of uranyl extraction in the dominant channel of Er-MOF at equilibrium after a 20 ns MD NVT simulation. The simulations suggest that all uranyl cations are preferentially captured by forming outer-sphere complexes on the wall of the channel, as shown in Figure 5b. This represents a new type of interaction of host carboxyl groups that is different from inner-sphere coordination of Th^{4+} ions in MOFs.[66] Uranyl evidently occupies sites previously occupied by $Me_2NH_2^+$ moieties. The water ligands of uranyl cations bridge uranyl and Er-MOF moieties via hydrogen bonding to the exposed oxygen acceptors from the framework carboxyl groups. The simulations support the conclusion that uranyl adsorption in the RE-MOFs occurs through an ion-exchange process, and are in accord with EXAFS results that suggest uranyl is coordinated by water in a similar manner as in aqueous solution.

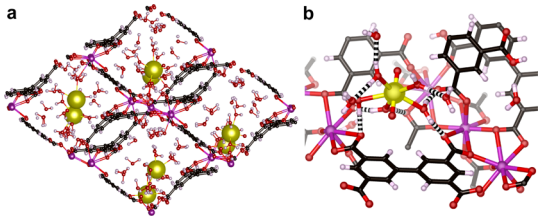

Figure 5. (a) MD simulations on the process of uranyl adsorption within the dominant channels of Er-MOF showing a snapshot of eight UO_2^{2+} cations adsorbed in a triclinic 2 × 2 × 2 supercell at equilibrium. (b) Snapshot to show the water-mediated outer-sphere of uranyl to the walls of channels. Black, pink, red, purple, and golden spheres represent C, H, O, Er, and U, respectively. Striped bonds represent hydrogen bonds between water ligands and oxygen donors of the framework.

CONCLUSIONS

This work reported an efficient strategy to develop novel anionic MOF adsorbents with high performance on uranium(VI) uptake. In addition to identifying the lanthanide contraction or metal node effect to be crucial for the adsorption properties of MOFs, uranium(VI) extraction on Y-MOF attains 538 mg/g at pH 3.0, representing one of the largest values for uranium(VI) capture by MOFs. Although the practical applications of RE-MOFs may be restricted by the expensive cost of RE metal, this work offers valuable clues for

rational construction of porous MOFs applied in metal ions' extraction. Further studies are underway to address practical issues of MOFs applied in metal adsorption and test other MOFs constructed by various metal nodes as promising scavenger materials of uranium(VI) and other actinide ions.

■ ASSOCIATED CONTENT

Supporting Information

The Supporting Information is available free of charge at https://pubs.acs.org/doi/10.1021/acsami.0c02121.

Preparation procedures and characterizations of RE-MOFs, uranium(VI) adsorption experiments and analyses details, and additional PXRD, IR, and MD simulations (PDF)

Crystallographic data for RE-MOFs (CCDC. nos. 1586753−1586759) (CIF)

Corresponding Authors

Li-Yong Yuan − *Laboratory of Nuclear Energy Chemistry, Institute of High Energy Physics, Chinese Academy of Sciences, Beijing 100049, China;* orcid.org/0000-0003-4261-8717; Email: yuanly@ihep.ac.cn

Wei-Qun Shi − *Laboratory of Nuclear Energy Chemistry, Institute of High Energy Physics, Chinese Academy of Sciences, Beijing 100049, China;* orcid.org/0000-0001-9929-9732; Email: shiwq@ihep.ac.cn

Authors

Zhi-Hui Zhang − *Jiangsu Key Laboratory of Advanced Catalytic Materials and Technology, Advanced Catalysis and Green Manufacturing Collaborative Innovation Center, Changzhou University, Changzhou 213164, China;* orcid.org/0000-0002-8744-7897

Jian-Hui Lan − *Laboratory of Nuclear Energy Chemistry, Institute of High Energy Physics, Chinese Academy of Sciences, Beijing 100049, China*

Pan-Pan Sheng − *Jiangsu Key Laboratory of Advanced Catalytic Materials and Technology, Advanced Catalysis and Green Manufacturing Collaborative Innovation Center, Changzhou University, Changzhou 213164, China*

Ming-Yang He − *Jiangsu Key Laboratory of Advanced Catalytic Materials and Technology, Advanced Catalysis and Green Manufacturing Collaborative Innovation Center, Changzhou University, Changzhou 213164, China*

Li-Rong Zheng − *Beijing Synchrotron Radiation Facility, Institute of High Energy Physics, Chinese Academy of Sciences, Beijing 100049, China*

Qun Chen − *Jiangsu Key Laboratory of Advanced Catalytic Materials and Technology, Advanced Catalysis and Green Manufacturing Collaborative Innovation Center, Changzhou University, Changzhou 213164, China*

Zhi-Fang Chai − *Laboratory of Nuclear Energy Chemistry, Institute of High Energy Physics and Engineering Laboratory of Advanced Energy Materials, Ningbo Institute of Industrial Technology, Chinese Academy of Sciences, Beijing 100049, China*

John K. Gibson − *Chemical Sciences Division, Lawrence Berkeley National Laboratory (LBNL), Berkeley, California 94720, United States;* orcid.org/0000-0003-2107-5418

Author Contributions

Z.-H.Z and J.-H.L. contributed equally. W.-Q.S. and Z.-F.C. conceived the project. Z.-H.Z., P.-P.S., and M.-Y.H. designed and performed the synthesis and characterizations. P.-P.S. and L.-Y.Y. performed the uranium extraction experiments. J.-H.L. performed the all-atom MD simulations. L.-Y.Y. and L.-R.Z. obtained and analyzed the EXAFS data. Z.-H.Z. and Q.C. recorded and analyzed the NMR data. Z.-H.Z., L.-Y.Y., J.K.G., and W.-Q.S. discussed the results and wrote the paper.

Notes

The authors declare no competing financial interest.

■ ACKNOWLEDGMENTS

This work was supported by the National Natural Science Foundation of China (grants nos 11775037, 21777161, 21836001, and 21806167) and Youth Innovation Promotion Association, CAS (2017020). The Science Challenge Project (TZ2016004) is also acknowledged. Z.-H.Z. acknowledges the Major Basic Research Project of the Natural Science Foundation of the Jiangsu Higher Education Institutions (grant 19KJA150001). Research of J.K.G. was supported by the Center for Actinide Science and Technology, an Energy Frontier Research Center funded by the U.S. Department of Energy, Office of Science, Basic Energy Sciences, under award number DE-SC0016568.

■ REFERENCES

(1) Eddaoudi, M.; Kim, J.; Rosi, N.; Vodak, D.; Wachter, J.; O'Keeffe, M.; Yaghi, O. M. Systematic Design of Pore Size and Functionality in Isoreticular MOFs and Their Application in Methane Storage. *Science* **2002**, *295*, 469−472.

(2) Gu, Z.-Y.; Yang, C.-X.; Chang, N.; Yan, X.-P. Metal-Organic Frameworks for Analytical Chemistry: From Sample Collection to Chromatographic Separation. *Acc. Chem. Res.* **2012**, *45*, 734−745.

(3) Chen, C.-X.; Wei, Z.-W.; Jiang, J.-J.; Zheng, S.-P.; Wang, H.-P.; Qiu, Q.-F.; Cao, C.-C.; Fenske, D.; Su, C.-Y. Dynamic Spacer Installation for Multirole Metal-Organic Frameworks: A New Direction toward Multifunctional MOFs Achieving Ultrahigh Methane Storage Working Capacity. *J. Am. Chem. Soc.* **2017**, *139*, 6034−6037.

(4) Luo, F.; Yan, C.; Dang, L.; Krishna, R.; Zhou, W.; Wu, H.; Dong, X.; Han, Y.; Hu, T.-L.; O'Keeffe, M.; Wang, L.; Luo, M.; Lin, R.-B.; Chen, B. UTSA-74: A MOF-74 Isomer with Two Accessible Binding Sites Per Metal Center for Highly Selective Gas Separation. *J. Am. Chem. Soc.* **2016**, *138*, 5678−5684.

(5) Jiang, J.; Furukawa, H.; Zhang, Y.-B.; Yaghi, O. M. High Methane Storage Working Capacity in Metal-Organic Frameworks with Acrylate Links. *J. Am. Chem. Soc.* **2016**, *138*, 10244−10251.

(6) Hartlieb, K. J.; Holcroft, J. M.; Moghadam, P. Z.; Vermeulen, N. A.; Algaradah, M. M.; Nassar, M. S.; Botros, Y. Y.; Snurr, R. Q.; Stoddart, J. F. Cd-MOF: A Versatile Separation Medium. *J. Am. Chem. Soc.* **2016**, *138*, 2292−2301.

(7) Herm, Z. R.; Wiers, B. M.; Mason, J. A.; van Baten, J. M.; Hudson, M. R.; Zajdel, P.; Brown, C. M.; Masciocchi, N.; Krishna, R.; Long, J. R. Separation of Hexane Isomers in a Metal-Organic Framework with Triangular Channels. *Science* **2013**, *340*, 960−964.

(8) Bloch, E. D.; Queen, W. L.; Krishna, R.; Zadrozny, J. M.; Brown, C. M.; Long, J. R. Hydrocarbon Separations in a Metal-Organic Framework with Open Iron(II) Coordination Sites. *Science* **2012**, *335*, 1606−1610.

(9) Li, P.; Vermeulen, N. A.; Gong, X.; Malliakas, C. D.; Stoddart, J. F.; Hupp, J. T.; Farha, O. K. Design and Synthesis of a Water-Stable Anionic Uranium-Based Metal-Organic Framework (MOF) with Ultra Large Pores. *Angew. Chem., Int. Ed.* **2016**, *55*, 10358−10362.

(10) Li, L.; Lin, R.-B.; Krishna, R.; Li, H.; Xiang, S.; Wu, H.; Li, J.; Zhou, W.; Chen, B. Ethane/Ethylene Separation in a Metal-Organic Framework with Iron-Peroxo Sites. *Science* **2018**, *362*, 443−446.
(11) Corma, A.; García, H.; Llabrés i Xamena, F. X. Engineering Metal Organic Frameworks for Heterogeneous Catalysis. *Chem. Rev.* **2010**, *110*, 4606−4655.
(12) Horcajada, P.; Serre, C.; Maurin, G.; Ramsahye, N. A.; Balas, F.; Vallet-Regí, M.; Sebban, M.; Taulelle, F.; Férey, G. Flexible Porous Metal-Organic Frameworks for a Controlled Drug Delivery. *J. Am. Chem. Soc.* **2008**, *130*, 6774−6780.
(13) Bobbitt, N. S.; Mendonca, M. L.; Howarth, A. J.; Islamoglu, T.; Hupp, J. T.; Farha, O. K.; Snurr, R. Q. Metal-Organic Frameworks for the Removal of Toxic Industrial Chemicals and Chemical Warfare Agents. *Chem. Soc. Rev.* **2017**, *46*, 3357−3385.
(14) Hu, Z.; Deibert, B. J.; Li, J. Luminescent Metal-Organic Frameworks for Chemical Sensing and Explosive Detection. *Chem. Soc. Rev.* **2014**, *43*, 5815−5840.
(15) Roy, S.; Chakraborty, A.; Maji, T. K. Lanthanide-Organic Frameworks for Gas Storage and as Magneto-Luminescent Materials. *Coord. Chem. Rev.* **2014**, *273*−*274*, 139−164.
(16) Yang, X.; Lin, X.; Zhao, Y.; Zhao, Y. S.; Yan, D. Lanthanide Metal-Organic Framework Microrods: Colored Optical Waveguides and Chiral Polarized Emission. *Angew. Chem., Int. Ed.* **2017**, *56*, 7853−7857.
(17) Wu, Y.-P.; Xu, G.-W.; Dong, W.-W.; Zhao, J.; Li, D.-S.; Zhang, J.; Bu, X. Anionic Lanthanide MOFs as a Platform for Iron-Selective Sensing, Systematic Color Tuning, and Efficient Nanoparticle Catalysis. *Inorg. Chem.* **2017**, *56*, 1402−1411.
(18) Meyer, L. V.; Schönfeld, F.; Müller-Buschbaum, K. Lanthanide Based Tuning of Luminescence in MOFs and Dense Frameworks - from Mono- and Multimetal Systems to Sensors and Films. *Chem. Commun.* **2014**, *50*, 8093−8108.
(19) Michaelides, A.; Skoulika, S.; Siskos, M. G. 2d and 3d Photoreactive Lanthanide MOFs of Trans,Trans-Muconic Acid. *Chem. Commun.* **2013**, *49*, 1008−1010.
(20) Efthymiou, C. G.; Kyprianidou, E. J.; Milios, C. J.; Manos, M. J.; Tasiopoulos, A. J. Flexible Lanthanide MOFs as Highly Selective and Reusable Liquid MeOH Sorbents. *J. Mater. Chem. A* **2013**, *1*, 5061−5069.
(21) Firmino, A. D. G.; Figueira, F.; Tomé, J. P. C.; Paz, F. A. A.; Rocha, J. Metal-Organic Frameworks Assembled from Tetraphosphonic Ligands and Lanthanides. *Coord. Chem. Rev.* **2018**, *355*, 133−149.
(22) Wong, N. E.; Ramaswamy, P.; Lee, A. S.; Gelfand, B. S.; Bladek, K. J.; Taylor, J. M.; Spasyuk, D. M.; Shimizu, G. K. H. Tuning Intrinsic and Extrinsic Proton Conduction in Metal-Organic Frameworks by the Lanthanide Contraction. *J. Am. Chem. Soc.* **2017**, *139*, 14676−14683.
(23) Karmakar, A.; Desai, A. V.; Ghosh, S. K. Ionic Metal-Organic Frameworks (iMOFs): Design Principles and Applications. *Coord. Chem. Rev.* **2016**, *307*, 313−341.
(24) Wei, Y.-S.; Hu, X.-P.; Han, Z.; Dong, X.-Y.; Zang, S.-Q.; Mak, T. C. W. Unique Proton Dynamics in an Efficient MOF-Based Proton Conductor. *J. Am. Chem. Soc.* **2017**, *139*, 3505−3512.
(25) Abney, C. W.; Mayes, R. T.; Saito, T.; Dai, S. Materials for the Recovery of Uranium from Seawater. *Chem. Rev.* **2017**, *117*, 13935−14013.
(26) Veliscek-Carolan, J. Separation of Actinides from Spent Nuclear Fuel: A Review. *J. Hazard. Mater.* **2016**, *318*, 266−281.
(27) Burns, P. C. U6+ Minerals and Inorganic Compounds: Insights into an Expanded Structural Hierarchy of Crystal Structures. *Can. Mineral.* **2005**, *43*, 1839−1894.
(28) Sun, Q.; Aguila, B.; Ma, S. Opportunities of Porous Organic Polymers for Radionuclide Sequestration. *Trends Chem.* **2019**, *1*, 292−303.
(29) Xiao, C.; Silver, M. A.; Wang, S. Metal-Organic Frameworks for Radionuclide Sequestration from Aqueous Solution: A Brief Overview and Outlook. *Dalton Trans.* **2017**, *46*, 16381−16386.
(30) Aguila, B.; Sun, Q.; Cassady, H.; Abney, C. W.; Li, B.; Ma, S. Design Strategies to Enhance Amidoxime Chelators for Uranium Recovery. *ACS Appl. Mater. Interfaces* **2019**, *11*, 30919−30926.
(31) Sun, Q.; Aguila, B.; Perman, J.; Ivanov, A. S.; Bryantsev, V. S.; Earl, L. D.; Abney, C. W.; Wojtas, L.; Ma, S. Bio-Inspired Nano-Traps for Uranium Extraction from Seawater and Recovery from Nuclear Waste. *Nat. Commun.* **2018**, *9*, 1644.
(32) Shen, Y.; Chu, N.; Yang, S.; Li, X.; Cao, H.; Tian, G. Quaternary Phosphonium-Grafted Porous Aromatic Framework for Preferential Uranium Adsorption in Alkaline Solution. *Ind. Eng. Chem. Res.* **2019**, *58*, 18329−18335.
(33) Zhang, L.; Pu, N.; Yu, B.; Ye, G.; Chen, J.; Xu, S.; Ma, S. Skeleton Engineering of Homocoupled Conjugated Microporous Polymers for Highly Efficient Uranium Capture Via Synergistic Coordination. *ACS Appl. Mater. Interfaces* **2020**, *12*, 3688−3696.
(34) Li, B.; Sun, Q.; Zhang, Y.; Abney, C. W.; Aguila, B.; Lin, W.; Ma, S. Functionalized Porous Aromatic Framework for Efficient Uranium Adsorption from Aqueous Solutions. *ACS Appl. Mater. Interfaces* **2017**, *9*, 12511−12517.
(35) Zhang, S.; Zhao, X.; Li, B.; Bai, C.; Li, Y.; Wang, L.; Wen, R.; Zhang, M.; Ma, L.; Li, S. "Stereoscopic" 2d Super-Microporous Phosphazene-Based Covalent Organic Framework: Design, Synthesis and Selective Adsorption Towards Uranium at High Acidic Condition. *J. Hazard. Mater.* **2016**, *314*, 95−104.
(36) Sun, Q.; Aguila, B.; Earl, L. D.; Abney, C. W.; Wojtas, L.; Thallapally, P. K.; Ma, S. Covalent Organic Frameworks as a Decorating Platform for Utilization and Affinity Enhancement of Chelating Sites for Radionuclide Sequestration. *Adv. Mater.* **2018**, *30*, 1705479.
(37) Yu, J.; Yuan, L.-Y.; Wang, S.; Lan, J.; Zheng, L.; Xu, C.; Chen, J.; Wang, L.; Huang, Z.; Tao, W.; Liu, Z.; Chai, Z.-F.; Gibson, J. K.; Shi, W.-Q. Phosphonate Decorated Covalent Organic Frameworks for Actinide Extraction: A Breakthrough under Highly Acidic Conditions. *CCS Chem.* **2019**, *1*, 286−295.
(38) Zhang, W.; Bu, A.; Ji, Q.; Min, L.; Zhao, S.; Wang, Y.; Chen, J. Pk(a) -Directed Incorporation of Phosphonates into MOF-808 Via Ligand Exchange: Stability and Adsorption Properties for Uranium. *ACS Appl. Mater. Interfaces* **2019**, *11*, 33931−33940.
(39) Yang, W.; Pan, Q.; Song, S.; Zhang, H. Metal-Organic Framework-Based Materials for the Recovery of Uranium from Aqueous Solutions. *Inorg. Chem. Front.* **2019**, *6*, 1924−1937.
(40) Xu, L.; Zhang, D.; Ma, F.; Zhang, J.; Khayambashi, A.; Cai, Y.; Chen, L.; Xiao, C.; Wang, S. Nano-MOF+ Technique for Efficient Uranyl Remediation. *ACS Appl. Mater. Interfaces* **2019**, *11*, 21619−21626.
(41) Wang, X.-F.; Chen, Y.; Song, L.-P.; Fang, Z.; Zhang, J.; Shi, F.; Lin, Y.-W.; Sun, Y.; Zhang, Y.-B.; Rocha, J. Cooperative Capture of Uranyl Ions by a Carbonyl-Bearing Hierarchical-Porous Cu-Organic Framework. *Angew. Chem., Int. Ed.* **2019**, *58*, 18808−18812.
(42) Zhang, X.; Liu, Y.; Jiao, Y.; Gao, Q.; Yan, X.; Yang, Y. Facile Construction of Fe@ Zeolite Imidazolate Framework-67 to Selectively Remove Uranyl Ions from Aqueous Solution. *J. Taiwan Inst. Chem. Eng.* **2018**, *91*, 309−315.
(43) Zhang, T.; Ling, B.-K.; Hu, Y.-Q.; Han, T.; Zheng, Y.-Z. An Anionic Manganese(II) Metal-Organic Framework for Uranyl Adsorption. *CrystEngComm* **2019**, *21*, 3901−3905.
(44) Wang, X.; Chen, L.; Wang, L.; Fan, Q.; Pan, D.; Li, J.; Chi, F.; Xie, Y.; Yu, S.; Xiao, C.; Luo, F.; Wang, J.; Wang, X.; Chen, C.; Wu, W.; Shi, W.; Wang, S.; Wang, X. Synthesis of Novel Nanomaterials and Their Application in Efficient Removal of Radionuclides. *Sci. China Chem.* **2019**, *62*, 933−967.
(45) Feng, Y.; Jiang, H.; Li, S.; Wang, J.; Jing, X.; Wang, Y.; Chen, M. Metal-Organic Frameworks HKUST-1 for Liquid-Phase Adsorption of Uranium. *Colloids Surf., A* **2013**, *431*, 87−92.
(46) Yang, W.; Bai, Z.-Q.; Shi, W.-Q.; Yuan, L.-Y.; Tian, T.; Chai, Z.-F.; Wang, H.; Sun, Z.-M. MOF-76: From a Luminescent Probe to Highly Efficient U-VI Adsorption Material. *Chem. Commun.* **2013**, *49*, 10415−10417.

(47) Bai, Z.-Q.; Yuan, L.-Y.; Zhu, L.; Liu, Z.-R.; Chu, S.-Q.; Zheng, L.-R.; Zhang, J.; Chai, Z.-F.; Shi, W.-Q. Introduction of Amino Groups into Acid-Resistant MOFs for Enhanced U(VI) Adsorption. *J. Mater. Chem. A* **2015**, *3*, 525−534.
(48) Li, L.; Ma, W.; Shen, S.; Huang, H.; Bai, Y.; Liu, H. A Combined Experimental and Theoretical Study on the Extraction of Uranium by Amino-Derived Metal Organic Frameworks through Post-Synthetic Strategy. *ACS Appl. Mater. Interfaces* **2016**, *8*, 31032−31041.
(49) Luo, B.-C.; Yuan, L.-Y.; Chai, Z.-F.; Shi, W.-Q.; Tang, Q. U(VI) Capture from Aqueous Solution by Highly Porous and Stable MOFs: UiO-66 and Its Amine Derivative. *J. Radioanal. Nucl. Chem.* **2016**, *307*, 269−276.
(50) Yuan, L.; Tian, M.; Lan, J.; Cao, X.; Wang, X.; Chai, Z.; Gibson, J. K.; Shi, W. Defect Engineering in Metal-Organic Frameworks: A New Strategy to Develop Applicable Actinide Sorbents. *Chem. Commun.* **2018**, *54*, 370−373.
(51) Carboni, M.; Abney, C. W.; Liu, S.; Lin, W. Highly Porous and Stable Metal-Organic Frameworks for Uranium Extraction. *Chem. Sci.* **2013**, *4*, 2396−2402.
(52) Xiong, Y. Y.; Li, J. Q.; Yan, C. S.; Gao, H. Y.; Zhou, J. P.; Gong, L. L.; Luo, M. B.; Zhang, L.; Meng, P. P.; Luo, F. MOF Catalysis of Fe-Ii-to-Fe-Iii Reaction for an Ultrafast and One-Step Generation of the Fe_2O_3@MOF Composite and Uranium(VI) Reduction by Iron(Ii) under Ambient Conditions. *Chem. Commun.* **2016**, *52*, 9538−9541.
(53) Zhang, L.; Wang, L. L.; Gong, L. L.; Feng, X. F.; Luo, M. B.; Luo, F. Coumarin-Modified Microporous-Mesoporous Zn-MOF-74 Showing Ultra-High Uptake Capacity and Photo-Switched Storage/Release of U^{VI} Ions. *J. Hazard. Mater.* **2016**, *311*, 30−36.
(54) Liu, W.; Dai, X.; Bai, Z.; Wang, Y.; Yang, Z.; Zhang, L.; Xu, L.; Chen, L.; Li, Y.; Gui, D.; Diwu, J.; Wang, J.; Zhou, R.; Chai, Z.; Wang, S. Highly Sensitive and Selective Uranium Detection in Natural Water Systems Using a Luminescent Mesoporous Metal-Organic Framework Equipped with Abundant Lewis Basic Sites: A Combined Batch, X-Ray Abadsorption Spectroscopy, and First Principles Simulation Investigation. *Environ. Sci. Technol.* **2017**, *51*, 3911−3921.
(55) Ye, J.; Bogale, R. F.; Shi, Y.; Chen, Y.; Liu, X.; Zhang, S.; Yang, Y.; Zhao, J.; Ning, G. A Water-Stable Dual-Channel Luminescence Sensor for UO_2^{2+} Ions Based on an Anionic Terbium(III) Metal-Organic Framework. *Chem.—Eur. J.* **2017**, *23*, 7657−7662.
(56) Janicki, R.; Mondry, A.; Starynowicz, P. Carboxylates of Rare Earth Elements. *Coord. Chem. Rev.* **2017**, *340*, 98−133.
(57) Zhang, L.; Song, T.; Xu, J.; Sun, J.; Zeng, S.; Wu, Y.; Fan, Y.; Wang, L. Polymorphic Ln(III) and Bptc-Based Porous Metal-Organic Frameworks with Visible, Nir Photoluminescent and Magnetic Properties. *CrystEngComm* **2014**, *16*, 2440−2451.
(58) Rappe, A. K.; Casewit, C. J.; Colwell, K. S.; Goddard, W. A.; Skiff, W. M. Uff, a Full Periodic-Table Force-Field for Molecular Mechanics and Molecular-Dynamics Simulations. *J. Am. Chem. Soc.* **1992**, *114*, 10024−10035.
(59) Pomogaev, V.; Tiwari, S. P.; Rai, N.; Goff, G. S.; Runde, W.; Schneider, W. F.; Maginn, E. J. Development and Application of Effective Pairwise Potentials for UO_2^{n+}, NpO_2^{n+}, PuO_2^{n+}, and AmO_2^{n+} (N=1, 2) Ions with Water. *Phys. Chem. Chem. Phys.* **2013**, *15*, 15954−15963.
(60) Berendsen, H. J. C.; Grigera, J. R.; Straatsma, T. P. The Missing Term in Effective Pair Potentials. *J. Phys. Chem.* **1987**, *91*, 6269−6271.
(61) Ryckaert, J.-P.; Ciccotti, G.; Berendsen, H. J. C. Numerical-Integration of Cartesian Equations of Motion of a System with Constraints - Molecular-Dynamics of N-Alkanes. *J. Comput. Phys.* **1977**, *23*, 327−341.
(62) Spek, A. L. Single-Crystal Structure Validation with the Program Platon. *J. Appl. Crystallogr.* **2003**, *36*, 7−13.
(63) Meng, Q.; Xin, X.; Zhang, L.; Dai, F.; Wang, R.; Sun, D. A Multifunctional Eu MOF as a Fluorescent pH Sensor and Exhibiting Highly Solvent-Dependent Adsorption and Degradation of Rhodamine B. *J. Mater. Chem. A* **2015**, *3*, 24016−24021.
(64) Kim, H. K.; Yun, W. S.; Kim, M.-B.; Kim, J. Y.; Bae, Y.-S.; Lee, J.; Jeong, N. C. A Chemical Route to Activation of Open Metal Sites in the Copper-Based Metal-Organic Framework Materials HKUST-1 and Cu-MOF-2. *J. Am. Chem. Soc.* **2015**, *137*, 10009−10015.
(65) Min, X.; Yang, W.; Hui, Y.-F.; Gao, C.-Y.; Dang, S.; Sun, Z.-M. Fe_3O_4@ ZIF-8: A Magnetic Nanocomposite for Highly Efficient UO_2^{2+} Adsorption and Selective UO_2^{2+}/Ln(3+) Separation. *Chem. Commun.* **2017**, *53*, 4199−4202.
(66) Zhang, N.; Yuan, L.-Y.; Guo, W.-L.; Luo, S.-Z.; Chai, Z.-F.; Shi, W.-Q. Extending the Use of Highly Porous and Functionalized MOFs to Th(IV) Capture. *ACS Appl. Mater. Interfaces* **2017**, *9*, 25216−25224.
(67) Feng, M.-L.; Sarma, D.; Qi, X.-H.; Du, K.-Z.; Huang, X.-Y.; Kanatzidis, M. G. Efficient Removal and Recovery of Uranium by a Layered Organic-Inorganic Hybrid Thiostannate. *J. Am. Chem. Soc.* **2016**, *138*, 12578−12585.